Journal of Engineering and Applied Sciences 11 (4): 751-759, 2016
ISSN: 1816-949X

Switching Characteristics of SOA-Assisted All-Optical Sagnac Interferometer Switch for Picosecond Pulses

[1]Vahdat Nazerian, [2]Alireza Taghavi Nasrabadi and [1]Iman Esmaili Pain Afrakoti
[1]Department of Electrical Engineering, University of Mazandaran, Babolsar, Iran
[2]Department of Electrical and Electronic Engineering,
Islamic Azad University, Saveh Branch, Saveh, Iran

Abstract: In this study, switching mechanism in all-optical Sagnac interferometer using Semiconductor Optical Amplifier (SOA) is studied numerically. The switching characteristics of this scheme are investigated for picosecond input pulses. SOA all non-linear gain compression effects are considered altogether simultaneously in All-Optical Sagnac Interferometer Switch (AOSIS). The effect of structural and input pulse parameters on the AOSIS operation are identified and analyzed. Simulation results show that some key parameters such as SOA unsaturated gain, control pulse energy and width, SOA length and loop asymmetry of this scheme should be selected (or designed) so that the best operating conditions for switching is satisfied. It was shown that control pulse characteristics have the most effect on switching operation. It was shown that effects of picosecond nonlinearities of SOA are very important on switching characteristics. Furthermore, use of picosecond input pulses caused to the improving switching windows shape and the increasing bandwidth which be useful for broadband applications.

Key words: All-Optical Sagnac Interferometer Switches (AOSIS), picosecond pulses, nonlinear effects, semiconductor optical amplifier, satisfied

INTRODUCTION

Increasing demand for more bandwidth and speed in modern telecommunications and therefore high bit rate applications caused to actuate the recent research into analysis of ultrashort optical pulses. One of the main characteristic of all optical networks is that information remains completely in the optical domain along the process path without Opto-Electrical (O/E) and Electro-Optical (E/O) conversions. The implementation of ultrahigh speed all-optical networks requires the design and development of all-optical switches as a key communication element. These switches will perform a set of critical network processing functions such as shift register with inverter (Zoiros *et al*., 2005), address recognition (Glesk *et al*., 1994), full adder (Poustie *et al*., 1999) and multi/demulti-plexing (Diez *et al*., 2001).

As a switching element, Semiconductor Optical (SOA) is a promising choice for their the attractive features such as fast switching time, low power consumption, compactness, high nonlinear properties and capability of large-scale integration. Playing the role of nonlinear element originates from the carrier depletion due to strong nonlinearity of the SOA (Connelly, 2002). Sagnac interferometer is a favorable structure for the switching purpose and has wide application in communication. The Sagnac interferometer is called with different names in publications such as Terahertz Optical Asymmetric Demultiplexer (TOAD) (Sokoloff *et al*., 1993) and Semiconductor Laser Amplifier in a Loop Mirror (SLALOM) (Eiselt *et al*., 1995). SOA-assisted All-Optical Sagnac Interferometer Switch (AOSIS) has the ability to do a set of logic functions. In very recent researches new applications based on SOA-assisted AOSIS in optical network and communication (Chattopadhyay, 2011; Papadopoulos and Zoiros, 2011; Gayen *et al*., 2012; Zoiros *et al*., 2011), designing optical logic gate and circuit (Chattopadhyay, 2012; Gayen *et al*., 2011a, b; Maity *et al*., 2012; Taraphdar *et al*., 2011; Chattopadhyay and Roy, 2013), pulse shaping (De Dios and Lamela, 2011) are defined.

The most SOA-based AOSISs and its applications presented so far are analyzed in picosecond regimes. In our research in compare to other published papers (Zoiros *et al*., 2005; Diez *et al*., 2001; Zoiros *et al*., 2011; Tang *et al*., 1998) following important characteristics are considered: Dependency of SOA's gain spectral peak shift to carrier density variations (Razaghi *et al*., 2009a), including Group Velocity Dispersion (GVD) effect in SOA model, simultaneous consideration of SOA's all fast process nonlinear effects. Analysis of effect of structural and input pulse parameters on the AOSIS operation.

Corresponding Author: Vahdat Nazerian, Department of Electrical Engineering, University of Mazandaran, Babolsar, Iran

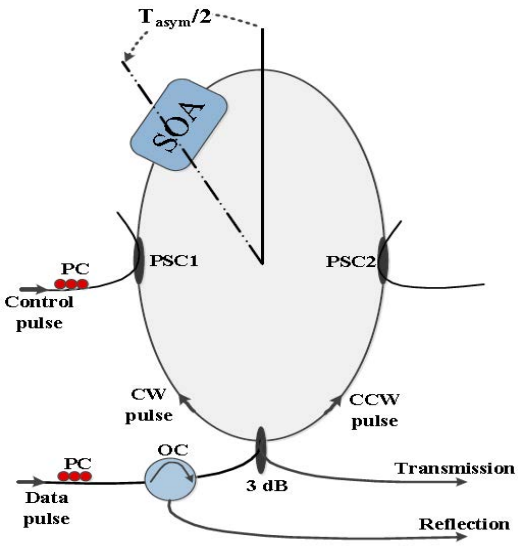

Fig. 1: Schematic structure of SOA-assisted AOSIS. OC: Optical Circulator, SOA: Semiconductor Optical Amplifier, PC: Polarization Controller, PSC: Polarization Selective Coupler

The proposed modeling scheme for SOA assisted of AOSIS, has the capability to predict realistic results in different complex all optical logic gates such as adder, inverter and flip-flop and so on (Chattopadhyay, 2011; Papadopoulos and Zoiros, 2011; Gayen *et al*., 2012; Zoiros *et al*., 2011; Chattopadhyay, 2012; Gayen *et al*., 2011a, b; Maity *et al*., 2012; Taraphdar *et al*., 2011; Chattopadhyay and Roy, 2012). Simulation results show that some key parameters such as SOA unsaturated gain, control pulse energy and width, SOA length and loop asymmetry of this scheme should be selected (or designed) so that the best operating conditions for switching is satisfied.

Principle of operation: The simplified schematic structure of the analyzed SOA-assisted AOSIS is shown in Fig. 1. The switch consists of an optical loop formed by the joint input and output ports of an independent 2×23 dB coupler and the SOA. The position of the SOA can be displaced asymmetrically respect to the center of loop by a distance that is equivalent to a temporal offset of $T_{asym}/2$ that can be achieved by using Optical Delay Line (ODL). When a data input light is entered into the loop through the input port, splits symmetrically to two counter-propagating pulses (the Clock Wise (CW) and Counter-Clock Wise (CCW)) with equal amplitudes. To discriminate the data from the high power control pulses in loop orthogonal polarizations for these pulses are adopted (for example, the control and data pulses with the Transverse Electric (TE) and Transverse Magnetic (TM) polarization vectors, respectively). Therefore, the control pulses can be inserted and extracted by means of two Polarization Selective Couplers (PSC) located in the loop.

Polarization Controllers (PC) role is adjusting control and data pulses polarization vectors so that both linearly polarized and aligned to the axes of the SOA. For each two time splitting of data pulses, 3 dB coupler induces a $\pi/2$ phase difference between its outputs lights. The propagation direction of data that is reflected back toward input port is changed by Optical Circulator (OC) to reflection output port. The induced phase difference between two data pulses (CW and CCW) due to propagation in wave guides that coupled 3dB coupler, PSC and SOA is assumed to be zero. The CW can be injected several picoseconds before or after the control pulse for different amounts of the asymmetric time delay (T_{asym}). T_{asym} cause to SOA nonlinearities the phase difference occurs between these two pulses. If the phase difference between these pulses reaches adequate amount (π) the input pulse will switched to transmission port in Fig. 1.

MATERIALS AND METHODS

Modeling: In order to theoretically explain the behavior of switching, the basic interferometric equations that describe the AOSIS operation and a comprehensive model to study sub-picosecond counter-propagation pulses in SOA are properly adopted to simulate SOA-assisted AOSIS behavior under various conditions.

AOSIS interferometric equations: Transfer function is the ratio of transmission or reflection output port power to the inserted data power. The basic interferometric equations that describe the output pulses at Transmission (T(t)) and Reflection (R(t)) ports can be written as (Dorren *et al*., 2002):

$$T(t)=\frac{P_{in}}{4}\left\{\begin{array}{l}G_{CW}(t)+G_{CCW}(t-T_{asym})-\\ 2\sqrt{G_{CW}(t)}G_{CCW}(t-T_{asym})\times\\ \cos\left[\phi_{CW}(t)-\phi_{CCW}(t-T_{asym})\right]\end{array}\right\} \quad (1)$$

And:

$$R(t)=\frac{P_{in}}{4}\left\{\begin{array}{l}G_{CW}(t)+G_{CCW}(t-T_{asym})-\\ 2\sqrt{G_{CW}(t)}G_{CCW}(t-T_{asym})\times\\ \cos\left[\phi_{CW}(t)-\phi_{CCW}(t-T_{asym})\right]\end{array}\right\} \quad (2)$$

where, $G_{CW}(t)$ and $G_{CCW}(t)$ are the SOA gain seen by the CW and CCW pulses and $G_{CW}(t)$ and $G_{CCW}(t)$ are the corresponding phase shifts. These two parameters are related to Δ_{NL} by:

$$\Delta\phi_{NL} = \phi_{CW}(t) - \phi_{CCW}(t) = -\frac{\alpha_N}{2}\mathrm{Ln}\left(\frac{G_{CW}(t)}{G_{CCW}(t)}\right) \quad (3)$$

where, α_N is the line width enhancement factor associated with the gain changes due to carrier depletion.

SOA model: Calculation of T(t) and R(t) through Eq. 1 and 2 requires to find the gains experienced by the counter-propagating data pulses. This in turn can be obtained by taking into account all nonlinear effects in the SOA for sub-picosecond pulses through Modified Nonlinear Schrödinger Equation (MNLSE) which should be solved numerically. The analysis is based on central difference approximation in time domain and trapezoidal integration technique for spatial steps (Hong *et al*., 1996). The forward and backward data and control optical fields with complex amplitude are determined by the following expression. The electrical fields is written as (Karnik, 1999b):

$$E(z,t) = A(z,t)\exp\left[-i(\omega_o t \mu \beta_o z)\right] \quad (4)$$

Where:

A = Slowly varying complex envelope function of a propagating optical pulse in the SOA length

$\omega_o/2\pi$ = The carrier frequency

β_o = The propagating constant in SOA at transparency

The envelop propagation is described by the well-known equation (Razaghi *et al*., 2009):

$$\frac{\partial A}{\partial z} + v_g^{-1}\frac{\partial A}{\partial t} = g(1 - i\alpha_N)A \quad (5)$$

Where:

v_g = Group velocity

α_N = Line width enhancement factor associated with the gain change due to carrier depletion

Due to relatively narrow spectral width of optical pulse, the field gain g is assumed to be frequency independent. Otherwise, g in Eq. 6 should be replaced by an operator including second order time derivative (Borri *et al*., 1999). The interaction between pulses and SOA is described by the following ordinary differential rate equation:

$$\frac{\partial g}{\partial t} = \frac{g_o - g}{\tau} - \frac{g \times |A|^2}{E_{sat}} \quad (6)$$

Where:

τ = Carrier lifetime

E_{sat} = Saturation energy of SOA. The small-signal gain coefficient per unit SOA length (linear gain)

g_0 = Determined by current injection

The parameters of a bulk SOA (InGaAsP/InP, double hetero-structure) is used at the center frequency 193.5 THz for the simulation. The length of the SOA is assumed to be 500 μm. We have obtained all the results with a propagation step Δz of 500/256 μm in the SOA.

RESULTS AND DISCUSSION

Here we consider all SOA's fast process effects simultaneously to calculate carrier dependent nonlinear gain for switching performance. In our simulation we use sech^2. Fourier transform limited data and control pulses. Figure 2 shows the data pulses gain, phase difference between CW and CCW pulses, extinction ratio (T(t)/R(t)) and normalized output power (T(t)/(R(t)+T(t))) as a function of the time delay (Td) between the CW and the control pulse. Physically, a negative value of the time delay means that the CW pulse is behind the control pulse while for positive time delay values control pulse is behind the CW pulse.

The time required for a data pulse to pass SOA's length is approximately 7 ps. T_{asym} = 3.5 ps that means CW pulse 3.5 ps a head of CCW pulse. As shown in Fig. 2a for small T_d, CW and control pulses propagates in a same time frame in SOA and will have most overlap in its waveguide. Due to this overlap, the SOA's gain will be saturated and CW pulse will be less amplified. For positive T_d, CW reaches SOA after control pulse and receives unsaturated SOA gain and hence will get higher gain respect to negative T_d. At T_d<-17.5 ps, the CCW is injected to SOA after control pulse and will receive saturated SOA's gain. By increasing T_d, CCW propagates in larger unsaturated SOA's length and therefore its output amplitude will increase.

The dip appeared at around T_d = 0 ps and T_d = -15 ps in CW and CCW gain profiles is due to the collision of CW and CCW pulses by control pulse inside SOA near corresponding facet, respectively. As shown in Fig. 2b when there is no delay between the data pulses (CW and CCW) the phase difference reaches π value. Fig. 2c and d show normalized power and extinction ratio profiles. As depicted in this Fig. 2, just for-1150 fs<T_d<150 fs period the normalized power is >0.9 and switching occurred. The

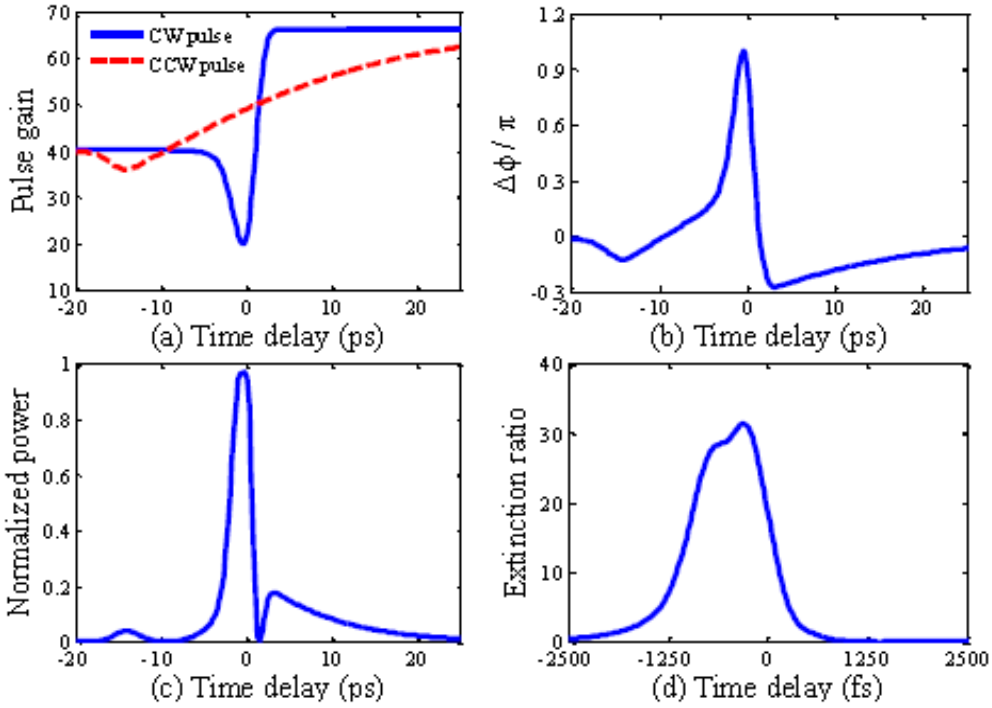

Fig. 2: a) Pulse gain; b) phase difference between CW and CCW pulses; c) normalized power (T(t)/(R(t)+T(t))) ;d) extinction ratio (T(t)/R(t)) versus time delay between the CW and the control pulse

maximum values of normalized power (0.97) and extinction ratio (32.3) are happened at T_d = -300 fs which are simultaneous with maximum phase difference ($\Delta\phi_{NL}/\pi$ = 1). As shown in Fig. 2, the switching windows due to use of short input data and control pulses is narrow (5 ps) and symmetric. This is helpful for high bit rate switching in SOA-assisted AOSIS devices.

Now, we discuss the switching characteristics of AOSIS for different operating conditions. Figure 3 illustrates (a) normalized power, (b) extinction ratio from transmission port versus time delay between CW and control pulses for different values of SOA unsaturated gain ($G_0 = \exp(g_0 L)$) and (c) normalized power versus G_0 for T_d = -300 fs. To induce the desired gain ratio (G_{CW}/G_{CCW}) and hence phase difference between the counter-propagating data pulses the SOA optical properties must be modified by control pulse. For this purpose, the control pulse power must be at least 10 times higher than that of data pulse power which means that G_0 = 10. Increasing of G_0 is due to increase of SOA linear gain (g_0) at fixed SOA Length (L). As shown in Fig. 3a and b, the best operation of AOSIS occurred for G_0 = 24 dB case. In this case, the π phase difference happened when control pulse injected 300 fs earlier than CW pulse to the SOA and hence the highest normalized average output power (0.97) and extinction ratio (31.4) will occur. For G_0 = 27 dB, the phase difference between data pulses exceeds from the π value. The double peaks of normalized power and extinction ratio for G_0 = 27 dB are in accordance with time delays that phase difference is π. For G_0 = 21 dB due to low unsaturated gain and the gain ratio (G_{CW}/G_{CCW}) the phase difference between data pulses won't reach π. Therefore, undesirable normalized power and low extinction ratio are achieved in this case. Based on Fig. 3b, only for-2500<T_d<1000 fs the switching window is opened and only for-1250<Td<100 fs switching is occurred. Figure 3c shows normalized power versus G_0 for Td = -300 fs. According to Fig. 3, best operation of switch is achieved around G_0 = 24 dB and only for 22 dB<G_0<25.5 dB interval switching is occurred.

Figure 4 shows the influence of control pulse energy (E_{cntrl}) on the switching characteristics of our proposed scheme. This is the energy required for achieving a differential phase shift between the counter-propagating data pulses. Therefore it leads to complete constructive interference at the Transmission port (for normalized power>0.9). Increasing control pulse energy leads to enhanced carrier depletion which in turn caused to less gain for each data pulses. In Fig. 4a for E_{cntrl} = 100 fJ case, the phase difference reaches π for T_d = -1450 fs and T_d = 250 fs time delays and exceed it for -1450<T_d<250 fs due to high control pulse energy. Double peaks in

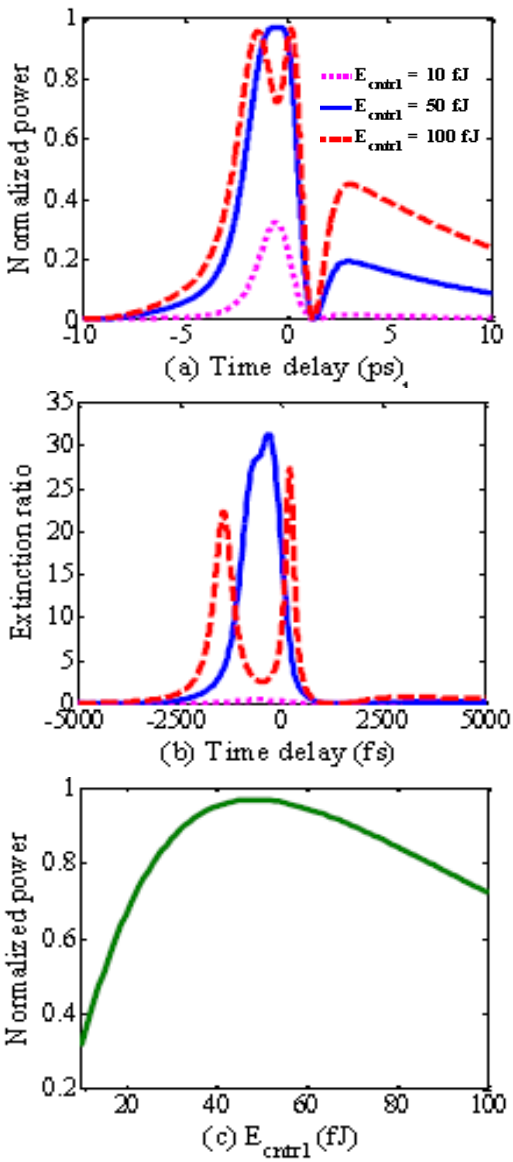

Fig. 3: a) Normalized power; b) Extinction ratio from transmission port versus time delay between CW and control pulses for different values of SOA unsaturated gain (G_0); c) Normalized power versus G_0 for T_d = -300 fs

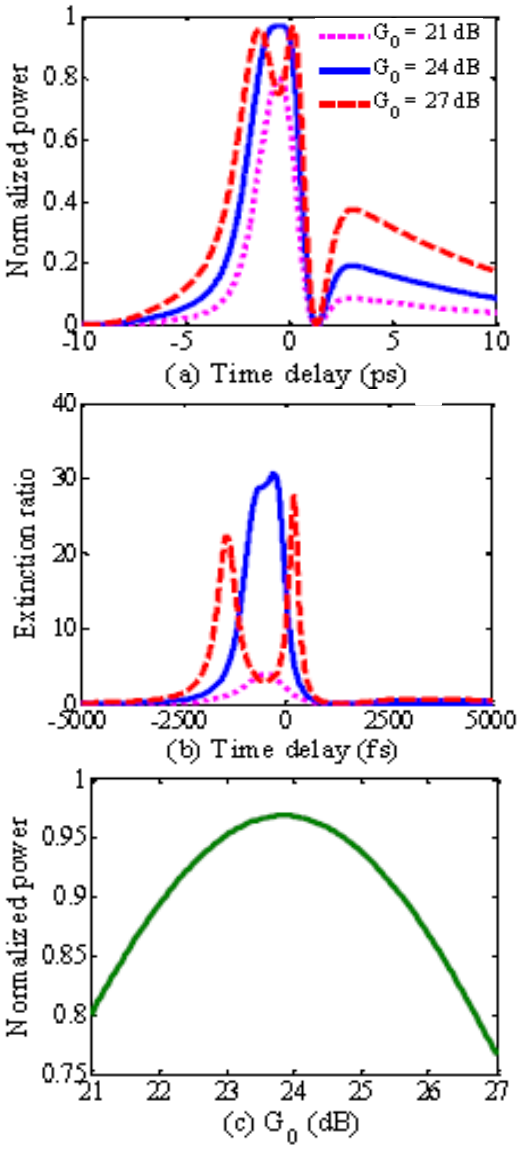

Fig. 4: a) Normalized power; b) Extinction ratio from transmission port versus time delay between CW and control pulses for different values of control pulse energy (E_{cntrl}); c) Normalized power versus E_{cntrl} for T_d = -300 fs

normalized power at two mentioned T_d values, demonstrates that 100 fJ is more than required value of control pulse power. Besides for E_{cntrl} = 10 fJ, the control pulse has very low energy and gain saturation don't occur and required phase difference will not reach. As shown in Fig. 4b for E_{cntrl} = 100 fJ, control pulse has enough energy to saturate SOA and hence the gains that data pulses receive will be less than in compare to E_{cntrl} = 50 fJ. It should be noted that based on Eq. 1 and 2, the maximum values of extinction ratio for E_{cntrl} = 100 fJ is less than E_{cntrl} = 50 fJ for certain time delays that corresponds to π phase difference between data pulses. Figure 4c shows normalized power versus E_{cntrl} for T_d = -300 fs. For low E_{cntrl}, control pulse energy is not enough to make phase difference of π and for high E_{cntrl}, control pulse energy phase difference will exceed from π. Therefore, switching occurs only for 35 <E_{cntrl}<70 fJ.

Figure 5 shows the effect of the control pulse duration, τ_{cntrl} on the switching operation. By decreasing

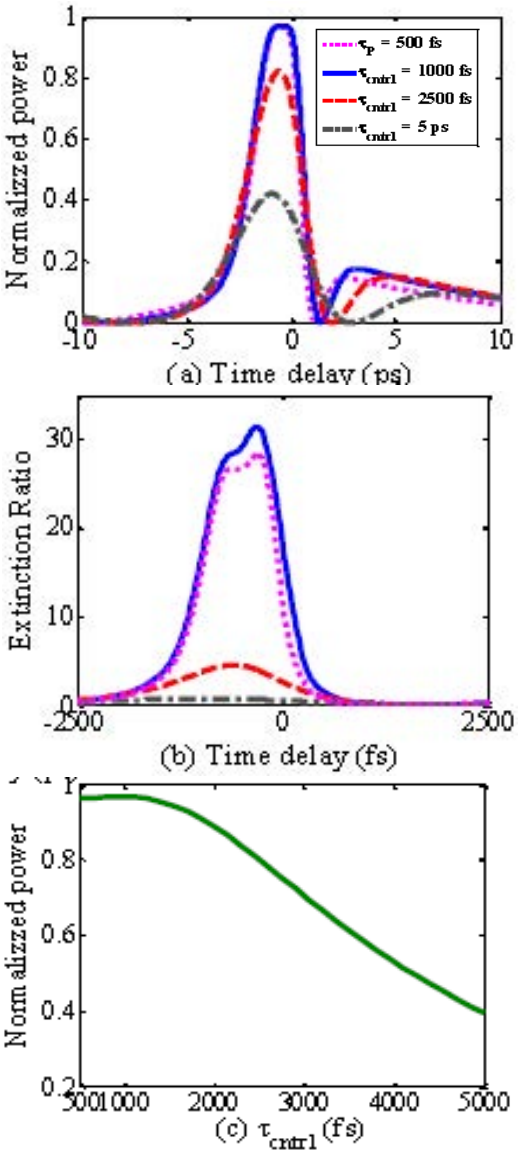

Fig. 5: a) Normalized power; b) extinction ratio from transmission port versus time delay between CW and control pulses for different values of control pulse width (τ_{cntrl}); c) Normalized power versus τ_{cntrl} for T_d = -300 fs

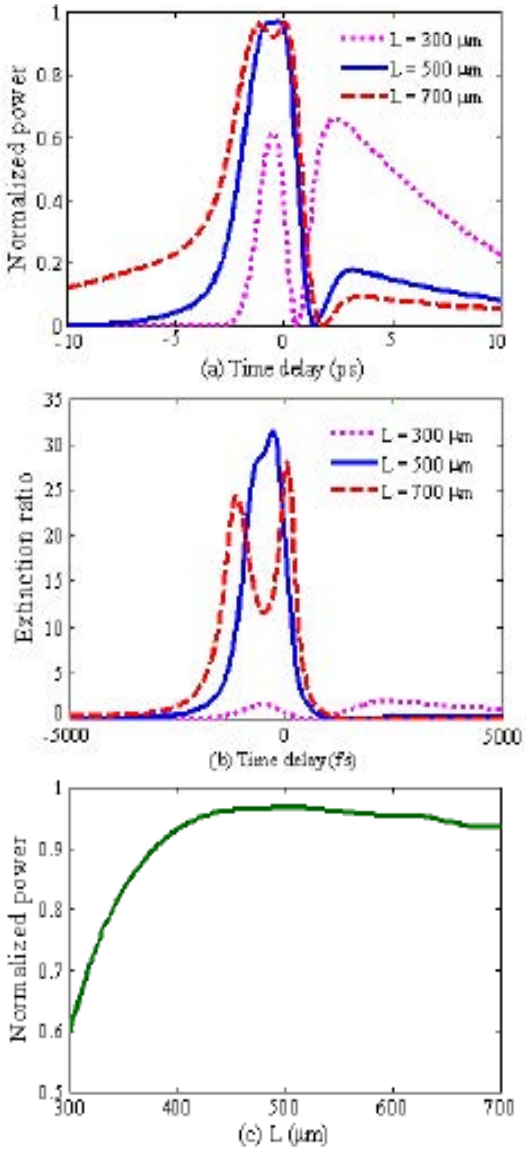

Fig. 6: a) Normalized power b) extinction ratio from transmission port versus time delay between CW and control pulses for different values of SOA Length (L); c) Normalized power for T_d =-300 fs versus L

of its pulse width it will remain less in SOA's waveguide this enhances the rapid depletion of carriers. At the fixed control pulse energy, the power of input pulse decreases inversely with the input data pulse width. As shown in Fig. 5a and b by increasing of control pulse width, required power for switching and hence transmission port power are decreased. For τ_{cntrl} = 500 and 1000 fs pulse widths control pulses have relatively the same behavior on switching characteristics but by increase of τ_{cntrl} normalized power and extinction ratio will decrease.

Figure 5b shows the normalized output power versus τ_{cntrl} for T_d = -300 fs. As shown in Fig. 5b, up to 1900 fs time delay, normalized power will be >0.9 and switching occurred. For T_d = 500 fs, phase difference is a little more than π for T_d = 1000 fs it reaches π and then by increasing control pulse width phase difference will be less than π. According to Fig. 5b, best operation of switch is achieved for T_d = 1000 fs.

To see the effect of structural parameters we will show the effect of SOA length and loop asymmetry (position of SOA in loop) on switch operation. Figure 6

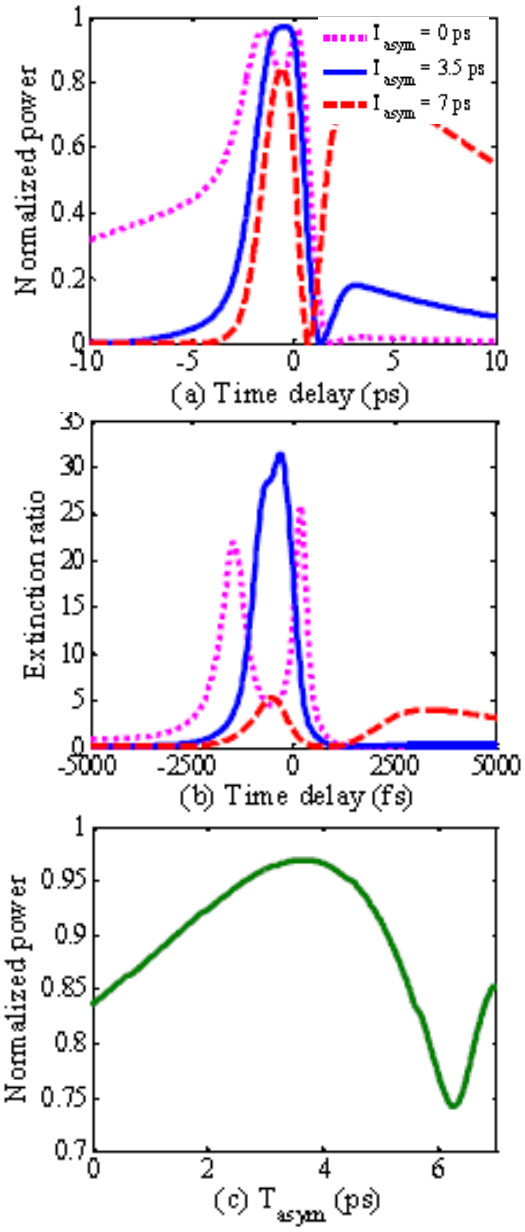

Fig. 7: a) Normalized power; b) Extinction ratio from transmission port versus time delay between CW and control pulses for different values of loop asymmetry (T_{asym}); c) Normalized power for T_d = -300 fs versus T_{asym}

shows the dependency of the switching characteristics on the SOA Length (L). SOA length affects the pulse propagation time in SOA waveguide and its gain it receive from SOA. The times required for a single pulse to pass from 700, 500 and 300 μm lengths of SOA are 10, 7 and 4.5 ps, respectively. As shown in Fig. 6a and b for L = 300 μm compared to two other lengths, the data pulses don't have enough time to reach required gain ratio and hence normalized power. For L = 700 μm due to long SOA cavity length, data pulses gain ratio is more than required amount and the phase difference will be exceed π. Consequently, double peaks at T_d =-1150 fs and T_d = 0 fs time delays in normalized power and extinction ratio for L = 700 μm are because at these two values of time delays phase difference reaches π. As shown in Fig. 6b due to proper CW and CCW pulses gain for L = 500 μm, its extinction ratio maximum value is higher than L = 700 μm. Figure 6c illustrates the optimum SOA length to have higher normalized output power for T_d = -300 fs. The result reveals that to have switching operation the SOA length should be >380 μm. As depicted in Fig. 6c the optimum gain ratio of data pulses occurs at L = 500 μm for fixed values of other parameters.

The switching characteristics variation versus the loop asymmetry or the asymmetric time delay (T_{asym}) is shown in Fig. 7. In this case increasing T_{asym} delays the CCW pulse arrival time to SOA and vice versa. As Fig. 7a indicates for T_{asym} = 0 ps data pulses reaches simultaneous to SOA. Therefore, the CCW pulse experiences more unsaturated SOA gain respect to T_{asym} = 3.5 ps and its gain increases, consequently gain ratio (G_{CW}/G_{CCW}) will be decreased. On the other hand for T_{asym} = 7 ps, the CCW pulse arrives at the SOA later than T_{asym} = 0 and 3.5 ps cases. For this T_{asym}, the CCW pulse experiences complete saturated SOA gain and its gain decreases, hence the gain ratio (G_{CW}/G_{CCW}) will be increased. By increase of gain ratio from required amount for two time delays phase difference reaches π and double peaks in normalized power and extinction ratio occurs. Figure 7c illustrates the optimum loop asymmetry to have higher normalized output power for T_d = -300 fs. As can be observed to have switching operation the loop asymmetry should be $1.4<T_{asym}<5.1$ ps and the optimum gain ratio of data pulses occurs around T_{asym} = 3.5 ps for fixed values of other parameters.

It can be concluded as it is shown in Fig. 3-7 the effect of several input parameters are exanimate and optimized condition for switching is obtained. Accordingly for best results this input parameters should be selected as follows: (a) Small signal gain, 24 dB, (b) Control pulse energy, 50 fJ, (c) Control pulse duration, 1000 fs, (d) SOA length, 500 μm and (e) loop asymmetry, 3.5 ps. It is shown in Fig. 3-7, the control pulse energy and its pulse width are the most important parameter that has considerable effect on the switch operation.

CONCLUSION

We have comprehensively investigated the switching characteristics of an SOA-assisted all-optical Sagnac interferometer configuration. A comprehensive

and computational improved finite-difference time-dependent beam propagation method was applied to solve modified nonlinear Schrodinger equations. These equations have the capability to describe the interaction between the sub-picosecond control and data pulses in the SOA as well as the output power variation caused by changing their time delay. Simulation studies show the effects of different structural and control pulse parameters on the switching operation of configuration.

For this reason, the dependencies of normalized output power and extinction ratio to the key input important parameters are investigated. Our simulation results were shown the optimum condition to extract maximum switching output power. It was shown that control pulse characteristics have the most effect on switching operation.

ACKNOWLEDGEMENTS

The researchers would like to give special thanks to University of Mazandaran, Department of Electrical Engineering for financial support to carry out this research.

REFERENCES

Borri, P., S. Scaffetti, J. Mork, W. Langbein, J.M. Hvam, A. Mecozzi and F. Martelli, 1999. Measurement and calculation of the critical pulsewidth for gain saturation in semiconductor optical amplifiers. Opt. Commun., 164: 51-55.

Chattopadhyay, T. and J.N. Roy, 2013. All-optical ordinary quaternary inverter (QNOT) using binary NOT gate. Optik-Int. J. Light Electron Opt., 124: 667-674.

Chattopadhyay, T., 2011. All-optical cross-bar network architecture using TOAD based interferometric switch and designing of reconfigurable logic unit. Opt. Fiber Technol., 17: 558-567.

Chattopadhyay, T., 2012. Terahertz Optical Asymmetric Demultiplexer (TOAD) based half-adder and using it to design all-optical flip-flop. Optik-Int. J. Light Electron Opt., 123: 1961-1964.

Connelly, M.J., 2002. Semiconductor Optical Amplifiers. Kluwer, Boston, MA., USA., ISBN-13: 9780792376576, Pages: 169.

De Dios, C. and H. Lamela, 2011. Improvements to long-duration low-power gain-switching diode laser pulses using a highly nonlinear optical loop mirror: Theory and experiment. J. Lightwave Technol., 29: 700-707.

Diez, S., E. Hilliger, M. Kroh, C. Schmidt and C. Schubert *et al*., 2001. Optimization of SOA-based Sagnac-interferometer switches for demultiplexing to 10 and 40 Gb/s. Opt. Commun., 189: 241-249.

Dorren, H.J.S., G.D. Khoe and D. Lenstra, 2002. All-optical switching of an ultrashort pulse using a semiconductor optical amplifier in a Sagnac-interferometric arrangement. Opt. Commun., 205: 247-252.

Eiselt, M., W. Pieper and H. Weber, 1995. SLALOM: Semiconductor laser amplifier in a loop mirror. J. Lightwave Technol., 13: 2099-2112.

Gayen, D., A. Bhattacharyya, R. Pal and J.N. Roy, 2011a. All-optical binary-coded decimal adder with a terahertz optical asymmetric demultiplexer. Comput. Sci. Eng., 13: 50-57.

Gayen, D.K., J.N. Roy, C. Taraphdar and R.K. Pal, 2011b. All-optical reconfigurable logic operations with the help of terahertz optical asymmetric demultiplexer. Optik-Int. J. Light Electron Opt., 122: 711-718.

Gayen, D.K., J.N. Roy and R.K. Pal, 2012. All-optical carry lookahead adder with the help of terahertz optical asymmetric demultiplexer. Optik-Int. J. Light Electron Opt., 123: 40-45.

Glesk, I., J.P. Solokoff and P.R. Prucnal, 1994. All-optical address recognition and self-routing in a 250 Gbit/s packet-switched network. Electron. Lett., 30: 1322-1323.

Hong, M.Y., Y.H. Chang, A. Dienes, J.P. Heritage, P.J. Delfyett, S. Dijaili and F.G. Patterson, 1996. Femtosecond self- and cross-phase modulation in semiconductor laser amplifiers. IEEE J. Sel. Top. Quantum Electron., 2: 523-539.

Karnik, A., 1999. Performance of TCP congestion control with rate feedback: TCP/ABR and rate adaptive TCP/IP. M. Eng. Thesis, Indian Institute of Science, Bangalore, India.

Maity, G.K., S.P. Maity and J.N. Roy, 2012. TOAD-based Feynman and Toffoli gate. Proceedings of the International Conference on Advanced Computing and Communication Technologies, January 7-8, 2012, Rohtak, Haryana, India, pp: 349-343.

Papadopoulos, G. and K.E. Zoiros, 2011. On the design of semiconductor optical amplifier-assisted Sagnac interferometer with full data dual output switching capability. Opt. Laser Technol., 43: 697-710.

Poustie, A.J., K.J. Blow, A.E. Kelly and R.J. Manning, 1999. All-optical full adder with bit-differential delay. Opt. Commun., 168: 89-93.

Razaghi, M., V. Ahmadi and M.J. Connelly, 2009a. Comprehensive finite-difference time-dependent beam propagation model of counterpropagating picosecond pulses in a semiconductor optical amplifier. J. Lightwave Technol., 27: 3162-3174.

Razaghi, M., V. Ahmadi and M.J. Connelly, 2009b. Femtosecond pulse shaping using counter-propagating pulses in a semiconductor optical amplifier. Opt. Quantum Electron., 41: 513-523.

Sokoloff, J.P., P.R. Prucnal, I. Glesk and M. Kane, 1993. A Terahertz Optical Asymmetric Demultiplexer (TOAD). IEEE Photon. Technol. Lett., 5: 787-790.

Tang, J.M., P.S. Spencer and K.A. Shore, 1998. Influence of fast gain depletion on the dynamic response of TOAD's. J. Lightwave Technol., 16: 86-91.

Taraphdar, C., T. Chattopadhyay and J.N. Roy, 2011. Designing of an all-optical scheme for single input ternary logical operations. Optik-Int. J. Light Electron Opt., 122: 33-36.

Zoiros, K.E., J. Vardakas, T. Houbavlis and M. Moyssidis, 2005. Investigation of SOA-assisted Sagnac recirculating shift register switching characteristics. Optik-Int. J. Light Electron Opt., 116: 527-541.

Zoiros, K.E., M.K. Das, D.K. Gayen, H.K. Maity, T. Chattopadhyay and J.N. Roy, 2011. All-optical pseudorandom binary sequence generator with TOAD-based D flip-flops. Opt. Commun., 284: 4297-4306.